INTERNATIONAL JOURNAL OF SUSTAINABLE ENGINEERING
2021, VOL. 14, NO. 5, 921–932
https://doi.org/10.1080/19397038.2021.1941392

Freshwater production by combination of solar still, earth-air heat exchanger and solar chimney for natural air draft

Salman H. Hammadi

Department of Mechanical Engineering, Engineering College, Basrah University, Basra, Iraq

ABSTRACT

A theoretical study of humidification-dehumidification (HDH) processes inside a system combining a solar still with an earth-air heat exchanger and a solar chimney was introduced. Energy and mass balances in a transient mode for the solar still and the earth-air heat exchanger in addition to the solar chimney were formulated and numerically simulated. The solar radiation heats water in the solar still basin, which in turn warms and humidifies dry air entering the solar still due to the heat and mass transfer into the airstream. When the glass/or the EAHE pipe wall temperatures are lower than or equal to the dew point of the humid air, the vapour condenses and runs down. The results show that the water, the air, and the glass temperatures increase with time to reach their maximum values (66.9 °C,61.8 °C, and 61.24 °C respectively) in June from 15.00 to 16.00. The humidity ratio along with the solar still length increases to reach a uniform value whenever the moist air is saturated. At the same time, the humidity ratio along EAHE decreases due to the condensation of the moisture inside the EAHE pipe. The condensation rate in the EAHE decreases gradually along a pipe length of 70 m until it completely vanishes at the pipe outlet. The hourly condensation rate in the EAHE attaining its *maximum value* of 49.27 kg/hr. at 14:32 (Basra local time) in June where the solar radiation is at maximum value. Also, the results indicated that the productivity of freshwater in the solar still is strongly affected by the water, air, and glass temperatures. The maximum productivity in the solar still achieved in March was 157 kg/day while it was 369 kg/day in July for the EAHE. The increase of the air velocity increases the productivity in EAHE and decreases it in the solar still. The daily average freshwater production for the system (solar still and the earth-air heat exchanger) throughout the year was found to be 207.44 kg. The thermal efficiency of the system over the interval from 6:00 to 19:00 was found to be 0.23–0.55. The economic evaluation showed that the cost of freshwater production was 0.0282 $/kg. A comparison of the current analysis with other works showed a good agreement.

ARTICLE HISTORY
Received 10 September 2020
Accepted 1 June 2021

KEYWORDS
Earth-air heat exchanger; open-type solar still; solar humidification-dehumidification

1.Introduction

The main objective of this study is to produce freshwater by using a combination system of a solar still and an external underground condenser with the benefit of a solar chimney for natural air motion of humid air through the system. Freshwater production is of vital importance especially in warm weather zones, which are known for having the highest water consumption for drinking, irrigation, and industrial activities. In remote areas, the energy transpose can prove to be quite difficult and costly; in this case, solar energy is considered the better alternative. Solar energy is widely used for desalination processes around the world most notably in the sunny and high solar intensity regions. A considerable number of researches available in the literature deals with a simple solar desalination system like solar still with some modifications to enhance the productivity of freshwater like Keshtkar, Eslami, and Jafarpur (1993), Abdullah et al. (2020), Zanganeh et al. (2020), Ali et al. (2020), Ayman and Hassan (2020). Several investigations found in the literature take the effect of air movement inside the solar still into account. Among these studies is the work by Ali (1991). He presented experimental research on-air motion effect inside a solar still of a 3 m^2 area to enhance the low yearly productivity of the still (3 L/ m^2 day). His results show a 29.7% increase in the desalinated water when the air is allowed to move inside the solar still. Also, Ali (1993) theoretically studied the effect of forced convection inside a solar still on heat and mass transfer coefficients bearing in mind the impact of turbulent air eddies, vapour velocity inside the still, and accumulation of non-condensable gas. He concluded that the productivity of the solar still increases with the increase of Reynold's number, but it falls after reaching a maximum value at Re = 52,800.

The freshwater extracted from the humid air in buried pipes is recently studied. Lindblom and Nordell (2006) studied a combined system for desalination and irrigation by underground condensation of moist air. They used solar radiation to evaporate seawater and let the humidified air transport into an underground pipe system. Their numerical simulations of this system result in water production of (1.8 kg/m. day) over a 50 m long pipe. Besides, Lindblom and Nordell (2007) extended their previous study by presenting a theoretical simulation on systems for drinking water production and for subsurface irrigation to examine the potential for using the condensation Irrigation (CI) technology. Their model used arrays of 50 m long pipes, spaced 1.0 m apart and buried at 0.5 m depth. They found that the mean water production rate

Salman H. Hammadi slmnhm@gmail.com Department of Mechanical Engineering, Engineering College, Basra University, Iraq

was 3.1 kg/m.day when they used drainage pipes for subsurface irrigation.

Recently Okati, Behzadmehr, and Farsad (2016) presented a study of a solar still including a compound system consisting of a solar humidifier and underground condenser. The amount of produced water per length of 0.2 diameter pipe buried in the ground is 3.8 kg/m.hr. Also, Okati, Farsad, and Behzadmehr (2018) extended their previous work by presented a numerical analysis of integrated humidification-dehumidification desalination unit and underground heat exchanger. Different numbers of buried pipes were taken, and the pipe wall temperature was considered as 17 °C. Their results indicated that the rate of water production could reach above 264.86 (kg/day) when they used an underground condenser of eight pipes (50 m length).

Ghazy and Fath (2016) studied solar desalination through a system that combined solar still and humidification-dehumidification unit. The main components of the system are a conventional solar still, humidifier, and dehumidifier. The moisture is extracted from the humid air in an external condenser(dehumidifier) that is cooled by water. Their simulation showed that the thermal efficiency and water production of the integrated system is about 1.5 times that of the conventional solar still under the same conditions. Bhargva and Yadav (2020) presented a theoretical and experimental study on a solar still combined with evacuated tubes and a heat exchanger. Experimental results showed maximum daily productivity of 7.38 L/m^2. day and daily efficiency of 30.5% achieved for modified still at 4 cm water depth. Sivaram et al. (2021) carried out an experimental study to produce clean water from any brackish water. Their study focused on the improvement in efficiency by providing a passive external condenser with a stepped design of evaporator. They showed that the passive external condenser increases the overall efficiency of still by 10.6% in summer and 12.2% in winter. Mohamed, Shahdy, and Ahmed (2021) performed a theoretical and experimental study of a solar humidification-dehumidification water desalination system based on a closed-air cycle. The impact of air flow rate, water to air mass ratio, and cooling water flow rate on water productivity have been investigated. Their experiments have been conducted at water temperatures of 40°C, 50°C, 60°C, and 70 °C. An increase in water temperature by 10 °C leads to an increase in freshwater production with an average of 69%. The results show that increasing air flow rate leads to increasing water productivity, while it reduces humidifier and dehumidifier efficiencies. They found that the maximum productivity was 6.32 kg/h at a cooling water flow rate of 6 kg/min.

The current study is a combination of a solar still, an earth-air heat exchanger, and a solar chimney. In this system, the solar radiation heats the water in the solar still basin, which in turn warms and humidifies the airstream due to heat and mass transfer from the water. A solar chimney is used to drive air through the solar still and the EAHE pipes. The freshwater will be extracted from the humid air by condensation of vapour in both the solar still and the earth-air heat exchanger. The previous studies available in the literature usually simplifying the mathematical model by neglecting the condensation on the glass cover of the solar still and considered only the condensation inside the buried pipes furthermore forced air circulation was used throughout the system. In the present work condensation on the glass cover which has significant productivity in the cold and moderate seasons as well as condensation in an earth-air heat exchanger is considered. A solar chimney is implemented for the natural movement of humid air in a zero-energy desalination system.

2. Theoretical analysis

2.1 The solar still

The solar still is a pool that has two openings, one to inlet dry air, and the second is to leave the humid air. The solar radiation incident on the solar still heated and humidified the air. The heat and mass transfer balances of the solar still depend upon whether condensation occurs on the glass cover or does not. If the temperature of the glass cover is equal to or below the dew point of the humid air, vapour will begin to condense on the glass cover (see Figure 1). The main assumptions used in the time-dependent mathematical model are:

1. One-dimensional flow in the entire system.
2. The solar still's basin and the solar chimney wall are perfectly insulated.
3. The soil temperature is a function of time and depth only.
4. The heat resistance of the buried pipe wall is neglected.

The energy balance of the solar still becomes:

$$Cp_f(T_{fo} - T_{fi}) + w_o h_{vo} - w_i h_{vi} = \frac{1}{\dot{m}_f}(q_{cw} + q_{ew} - q_{cg} - q_{eg}) \tag{1}$$

In the case of no condensation, the term (q_{eg}) which represents the latent heat released is zero.

The four terms of the right side of equation (1) are given as:

$$q_{cw} = h_w A(T_w - T_f) \tag{2}$$

$$q_{ew} = \frac{h_w}{Cp_f} A h_{fg}(w_w - w_f) \tag{3}$$

$$q_{cg} = h_f A(T_f - T_g) \tag{4}$$

$$q_{eg} = \frac{h_f}{Cp_f} A h_{fg}(w_f - w_g) \tag{5}$$

The humidity ratio at the water temperature of equation (3) is determined as: (Amer et al. 2009).

$$w_w = 0.622 \frac{P_{ws}}{P - P_{ws}} \tag{6}$$

The saturated vapour pressure P_{ws} in equation (6) is expressed as follows:(Sharshir et al. 2016),

Elango, Gunasekaran, and Sampathkumar 2015).

$$P_{ws} = \exp(25.317 - \frac{5144}{T_w + 273} \tag{7}$$

The humidity ratio of air is given as: (Hamed et al. 2015).

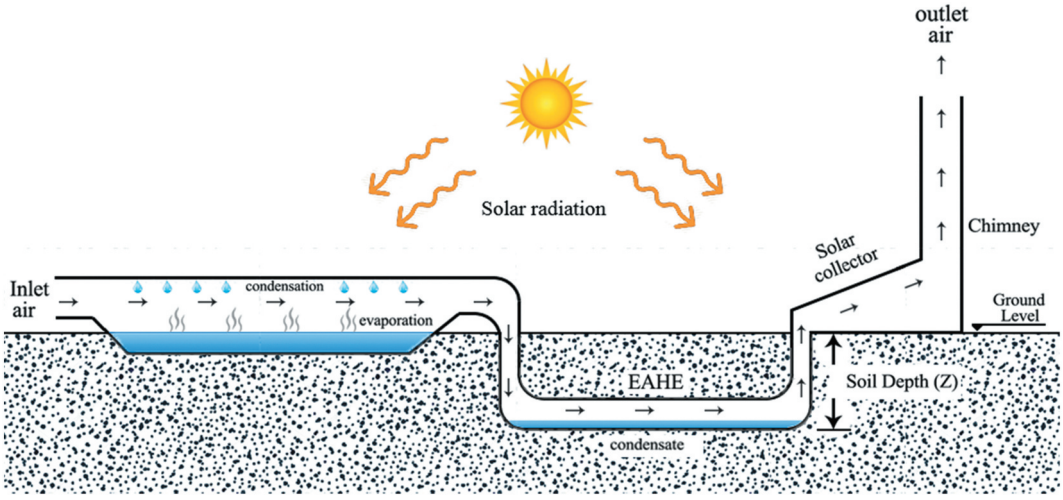

Figure 1. The physical model.

$$w_f = 0.622\frac{\emptyset P_f}{P - \emptyset P_f} \tag{8}$$

Where P_f is the saturated pressure at the air temperature, which is expressed as follows:

$$P_f = \exp(25.317 - \frac{5144}{T_f + 273} \tag{9}$$

The humidity ratio at the glass temperaturew_g in equation (5) is given as:

$$w_g = 0.622\frac{P_g}{P - P_g} \tag{10}$$

Where P_g is saturated pressure at the glass temperature, which is given as:

$$P_g = \exp(25.317 - \frac{5144}{T_g + 273} \tag{11}$$

The heat transfer coefficients for water – airstream h_w and airstream-glass cover h_f are considered as follows:(Okati, Farsad, and Behzadmehr 2018; Sartori 2006).

$$h_w = h_f = 2.8 + 3U_f \tag{12}$$

The latent heat of water vapour is given as: (Okati, Behzadmehr, and Farsad 2016; Rogers and Yau 1989).

$$h_{fg} = 1000\left(2500.8 - 2.36T_f + 0.0016{T_f}^2 - 0.00006{T_f}^3\right) \tag{13}$$

The enthalpy of saturated vapour at air temperature can be determined as: (Okati, Farsad, and Behzadmehr 2018),

Cengel and Boles 2001).

$$h_g = 1000\left(2501.3 + 1.82T_f\right), h_v \cong h_g \tag{14}$$

The humidity ratio for each element of dx length along with the solar still can be calculated from the mass balance equation as follows:

$$w_{n+1} = w_n + \frac{\dot{m}_{ev} - \dot{m}_{co}}{\dot{m}_f} \tag{15}$$

The evaporation and condensation rates$\dot{m}_{ev}, \dot{m}_{co}$ are given as: (Molineaux, Lachal, and Guisan 1994; Okati, Farsad, and Behzadmehr 2018).

$$\dot{m}_{ev} = \frac{h_w}{Cp_f} A\left(w_w - w_f\right) \tag{16}$$

$$\dot{m}_{co} = \frac{h_f}{Cp_f} A\left(w_f - w_g\right) \tag{17}$$

The dew point of the humid air is given by:(Lawrence 2005).

$$T_{dp} = \frac{243.04\left[\left[\ln\emptyset + \frac{17.625T_f}{243.04+T_f}\right]\right.}{17.625 - \ln\emptyset - \frac{17.625T_f}{243.04+T_f}} \tag{18}$$

The glass temperature that appeared in equation (4) can be determined using the energy balance for the glass cover as follows:

$$I\left(1 - \tau_g\right)\alpha_g + h_f\left(T_f - T_g\right) + \frac{h_f}{Cp_f} h_{fg}\left(w_f - w_g\right) = h_a\left(T_g - T_a\right) \tag{19}$$

The outside heat transfer coefficient h_a is given as: (Hassan, Elsherbiny, and Ghazy 2004; Hammadi 2018).

$$h_a = 5.7 + 3.8U_a \tag{20}$$

If no condensation on the glass ($T_g > T_{dp}$); the term $\frac{h_f}{Cp_f} h_{fg}\left(w_f - w_g\right)$ is eliminated from equation (19).

2.1.1 Solar radiation and ambient temperature

The total solar radiation incident on a horizontal surface estimated by curve fitting of data presented by Al-Enezi, Sykulski, and Nabil (2011):

$$I_{max} = 0.3967N^4 - 9.5368N^3 + 53.827N^2 + 41.119N + 407.29 \tag{21}$$

Where N is the month number.

The hourly solar radiation incident on the solar still is given as: (Hammadi 2018; Chaabene and Annabi 1997; Mawire and McPherson 2008).

$$I = I_{max} sin \frac{\pi t}{S} \tag{22}$$

Where S is the day length, which can be estimated from the following relation: (Besharat, Dehghan, and Faghih 2013).

$$S = \frac{2}{15} cos^{-1}[-\tan(\delta)\tan(L)] \tag{23}$$

The declination angle is given as:(El Mghouchi et al. 2016).

$$\delta = 23.45\sin[0.986(j + 284)] \tag{24}$$

The hourly ambient temperatureT_a throughout the day which appears in equation (19) is determined using the following formulas:(Reicosky et al. 1989).

For day

$$T_a = T_{a,min} + \left(T_{a,max} - T_{a,min}\right) \sin\left(\frac{\pi t}{S + 3.6}\right) \tag{25}$$

For night

$$T_a = T_{a,min} + \left(T_{sunset} - T_{a,min}\right) \exp\left(-2.2\frac{t - S}{24 - S}\right) \tag{26}$$

2.1.2 Evaluation of air temperature and humidity ratio

Equations (1, 15, and 19) can be solved numerically to evaluate the air temperature and humidity ratio along with the solar still length. If the glass temperature is higher than the dew point of the air, no condensation will occur, and the termsq_{eg} and $\frac{h_f}{Cp_f} h_{fg}\left(w_f - w_g\right)$ are eliminated from equations 1 and 19 respectively. The water temperature in the solar still basin $T_w$varies with the variation of solar intensity throughout the day. It can be calculated from the following time-dependent energy balance of the water layer:

$$M_w C_w \frac{dT_w}{dt} = I\alpha_w \tau_g A - h_w A\left(T_w - \bar{T}_f\right) - \frac{h_w}{Cp_f} A h_{fg}\left(w_w - \bar{w}_f\right) \tag{27}$$

The average air temperature and humidity ratio for any time interval along with the solar still can be determined numerically using the following relations:

$$\bar{T}_f(t) = \frac{1}{L}\int_0^L T_f(x)dx \tag{28}$$

$$\bar{w}_f(t) = \frac{1}{L}\int_0^L w_f(x)dx \tag{29}$$

2.2 Earth -Air heat exchanger model

After the humid air leaves the solar still, it enters the EAHE pipes. If the pipe wall temperature is equal to or less than the dew point of the air, condensation will occur and release the latent heat as well as to the sensible heat due to the temperature difference between the air and the pipe wall. The energy balance of the earth-air heat exchanger considered is written as:

$$Cp_f(T_{fi} - T_{fo}) + w_i h_{vi} - w_o h_{vo} = \frac{1}{\dot{m}_f}(q_{cp} + q_{ep}) \tag{30}$$

The convective heat transfer from the air to the pipe is:

$$q_{cp} = h_f A_p\left(T_f - T_p\right) \tag{31}$$

The heat released by condensation can be expressed as:

$$q_{ep} = \rho_f A_p h_m h_{fg}\left(w_f - w_p\right) \tag{32}$$

For constant wall temperature, the dimensionless mass transfer coefficient(Sh) depends on the flow type. In the case of laminar flow, it can be given as: (Çengel and Ghajar 2015).

$$Sh = 3.66 \tag{33}$$

For turbulent flow, (Sh) number is: (Estrada et al. 2018).

$$Sh = 0.023 Re^{0.8} Sc^{0.3} \tag{34}$$

The mass transfer coefficient $(h_m)$is expressed by: (Incropera 2006).

$$h_m = \frac{ShD_{ab}}{D_p} \tag{35}$$

Where $h_m$can be expressed in term of h_f as follows: (Çengel and Ghajar 2015).

$$h_{f=}\rho_f C_{pf} h_m \tag{36}$$

Where; D_{ab} is the mass diffusivity, which is given by: (Çengel and Ghajar 2015).

$$D = 1.8 \times 10^{-10} T_f^{2.072} \tag{37}$$

The humidity ratio for each element along with the length of the earth–air heat exchanger, is expressed as:

$$w_{f(n+1)} = w_{f(n)} - \frac{\dot{m}_{cp}}{\dot{m}_f} \tag{38}$$

The condensation rate in the EAHE is:

$$\dot{m}_{cp} = \frac{q_{ep}}{h_{fg}} \tag{39}$$

If no condensation, the air temperature in the EAHE can be determined by integrating equation (30) to give:

$$T_{f(z)} = T_p + \left(T_{fi} - T_p\right) Exp\left(\frac{-h_f \pi D_p z}{\dot{m}_f C_{pf}}\right) \tag{40}$$

The soil temperature for any depth at any time can be evaluated using the following formula: (Ozgener, Ozgener, and Tester 2013).

$$T_s(y,t) = T_m - A_s Exp\left[-y\left(\frac{\pi}{8760\alpha}\right)^{0.5}\right] \cos\left\{\frac{2\pi}{8760}\left[t - t_o - \frac{y}{2}\left(\frac{8760}{\pi\alpha_s}\right)^{0.5}\right]\right\} \tag{41}$$

The values of T_m, A_s, α_s and t_o are taken as 27 °C, 13.3 °C, 0.0038 m^2/hr, and 552 hr respectively, therefore, the last equation becomes [33]: (Al-Ajmi, Loveday, and Hanby 2006).

$$T_s(y,t) = 27 - 13.3Exp(-0.31y)\cos\left\{\frac{2\pi}{8760}(t - 552 - 428.31y)\right\} \quad (42)$$

In the current work, the pipe wall temperature T_p is taken equal to the soil temperature. This assumption has been addressed by (De Paepe and Janssens 2003) and (Fuxin et al. 2015).

2.3 Solar chimney

A simple energy balance equation for the solar chimney is written as follows;

$$\alpha_g I A_{co-} h_a A_{co}(T_{co} - T_a) = \dot{m}_f C_{pf}(T_{co} - T_f) \quad (43)$$

The updraught air velocity in the chimney is given by: (Bassiouny and Koura 2008).

$$u_f = cd\sqrt{\frac{gH_{ch}(T_{co} - T_f)}{T_f}} \quad (44)$$

Where the mass flow rate can be expressed as:

$$\dot{m}_f = \rho_f u A_{ch} \quad (45)$$

Using equations (43, 44, and 45), the air velocity in the chimney becomes:

$$\frac{\alpha I cd^2 g H_{ch}}{T_{fo}} - \frac{\rho_{fC_{pf}A_{ch}u^3}}{A_{co}} - u^2 h_a = 0 \quad (46)$$

The value of discharge coefficient (cd) is taken as 0.57 (Bassiouny and Koura 2008; Jianliu and Weihua 2013). Equation (46) can be easily solved numerically to evaluate the air velocity in the solar chimney at any time.

The solar radiation and the ambient temperature are taken according to Basra climate conditions (latitude 30.5, longitude 47.8) throughout the year. Equation (27) was solved numerically using the Euler method with a time interval of (300 seconds) to evaluate the water temperature as a function of the local time. The equations (1, 15, and 19) are resolved to evaluate air temperature and humidity ratio at any time for any location along with the solar still length.

2.4. Experimental validation

To validate the present theoretical model with other experimental and numerical works, the water temperature and the evaporation rate in the solar still throughout a time interval of 4:00–24.00 are compared with the results of Sartori (1996) and Okati, Farsad, and Behzadmehr (2018) in Table 1. The changes in the water temperature and the evaporation rate are similar in the three works. This indicates the validity of the present work results.

3. Results and discussion

A combination of a solar still, earth-air heat exchanger system and the solar chimney was analysed under Basra climate conditions (south of Iraq). Table 2 tabulated all the inlet parameters utilised in the calculations. The solution procedure includes simultaneous solving of the governing equations of the solar still, the earth-air heat exchanger, and the solar chimney. The solar still channel was divided into small elements of 0.1 m in length. The solution covered the entire length of the solar still for a time interval of 300s to determine the temperature, the humidity ratio, and the other heat and mass transfer characteristics. The air that leaves the solar still enters the earth-air heat exchanger where heat and mass transfer from the humid and warm air to the wall of the pipes. The EAHE pipes were divided into small elements of 0.1 m in length. The solution included checking whether condensation occurs on the EAHE pipes or not, depends on the dew point of the air and the temperature of the pipe's wall. The air temperature, humidity ratio, and condensation rate along the EAHE are calculated by solving equations (30) and (38) simultaneously.

The air is then drawn up through the solar chimney where the air velocity is calculated by solving equation (46) numerically. The water temperature in the solar still now can be estimated by solving the time-dependent equation (27) using the Euler method. The procedure is repeated for the next time interval and continues to cover a period from sunrise to midnight for each month around the year. All calculations are performed by building a program using the Matlab platform.

3.1 Variation of temperature

Figure 2 shows the water, the average air, and the average glass temperature profiles of the solar still during June. It is clear that the temperatures increase with time to reach maximum values at an interval between 15.00 and 16.00 then they start to go down. Such behaviours are due to the variation of the solar radiation incident on the solar still during the day. The air temperature along EAHE at the four seasons of the year is

Table 1. Experimentally and numerically validation of the present work with Sartori (1996) and Okati, Farsad, and Behzadmehr (2018) works.

	Time(hr.)	4–6	6–8	8–10	10–12	12–14	14–16	16–18	18–20	20–22	22–24
Water temperature (°C)	Sartori(Exp.)	24	24	35	58	63	66	53	39	34	29
	Okati(Num.)	26	25	25	34	55	62	66	56	49	43
	Present work	27	30	39	51	61	66	65	60	54	49
Evaporation rate kg/m^2 hr.	Sartori(Exp.)	0.05	0.04	0.1	0.42	0.64	0.6	0.42	0.22	0.18	0.16
	Okati	0.07	0.06	0.05	0.16	0.5	0.68	0.62	0.54	0.42	0.34
	Present work	0.012	0.011	0.036	0.22	0.53	0.81	0.8	0.59	0.41	0.29

Table 2. Inlet parameters.

Parameter	value
Width of the solar still	1 m
height of the solar still	0.5 m
Wind velocity	3 m/s
Inlet relative humidity	10%
Water absorptivity	0.9
glass absorptivity	0.1
Air specific heat	1005 J/kg K
Water density	1000 kg/m^3
Water specific heat	4200 J/kg K
Water layer height	0.08 m
Latitude	30.5°
Longitude	47.8°
EAHE length	70 m
EAHE diameter	0.25 m
Soil depth	5 m
Number of pipes	4
Chimney height	8 m
Collector area	50 m^2
Discharge coefficient	0.57

shown in Figure 3. The temperature gradually decreases with the EAHE length due to the sensible and latent heat removal from the air to the wall of the pipe. In all cases, the air temperature ultimately converges to the pipes wall temperature, or in other words, to the soil temperature, which are 24 °C, 26 °C, 30 °C, and 28 °C, in March, June, September, and December, respectively.

3.2 Humidity ratio

Figure 4 explains the change of humidity ratio along with the solar still length at different times. The humidity ratio increases along with the solar still length due to the mass transfer from the water to the airstream. It is noted that the humidity ratio decreases with time over the major part of the solar still and reaching a uniform value faster at t = 18.00, because of reducing the solar radiation, which leads to lower water temperature and less evaporation potential. Figure 5 shows a decrease in the humidity ratio along the EAHE due to the continuous condensation process. Besides, the humidity ratio decreases with time due to the reduction in the evaporation rate as the solar radiation and water temperature decrease.

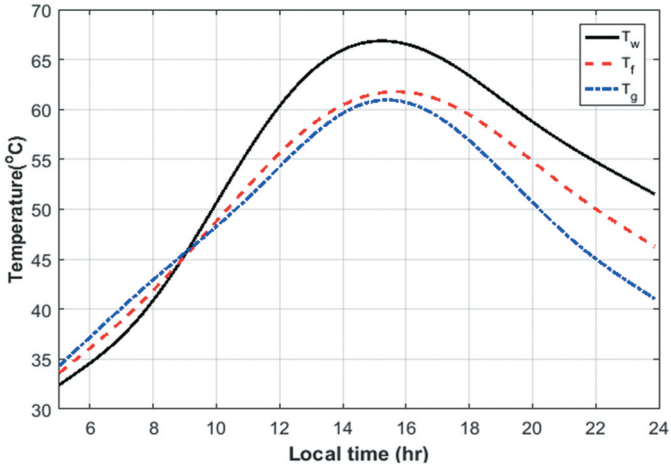

Figure 2. Air, water, and glass temperatures variation with time for the solar distiller.

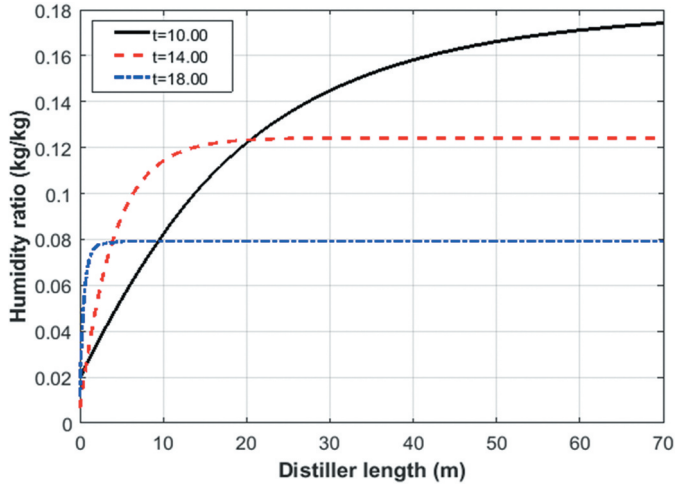

Figure 4. Humidity ratio profile for different times along the solar distiller.

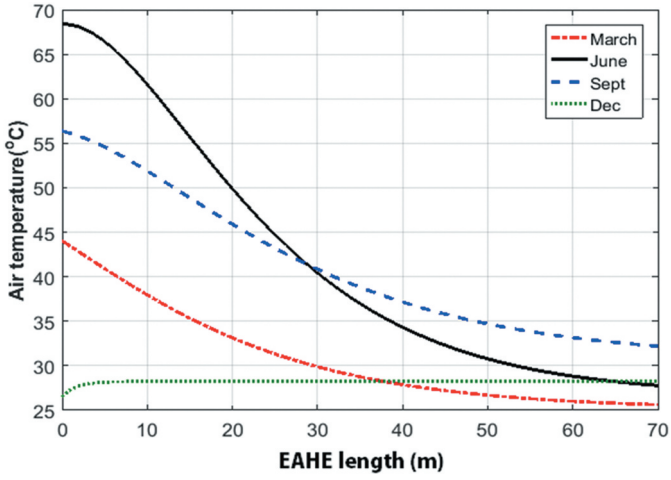

Figure 3. Air temperature profile for different months along the earth-air heat exchanger.

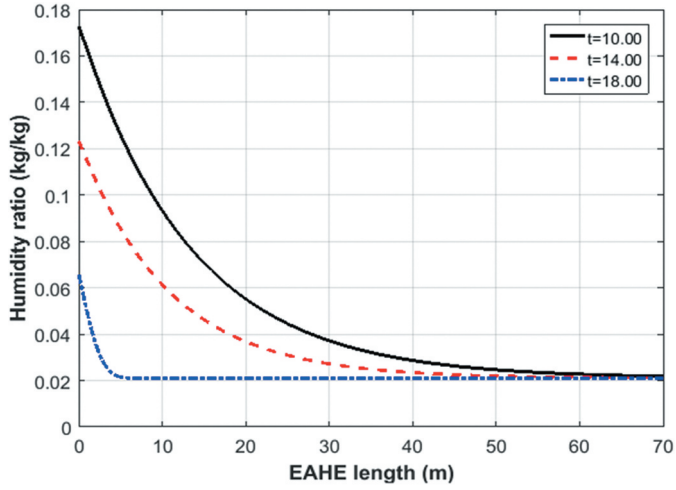

Figure 5. Humidity ratio profile for different times along the earth-air heat exchanger.

3.3 Condensation rate in EAHE

Figure 6 shows a decrease in condensation rate along the EAHE as the moisture content decreases due to the continuous condensation along the pipes. The condensation rate in June is the highest due to the increase of evaporation rate in the solar still where the maximum solar radiation exceeds 1000 W/m^2, which is the highest over the year. Figure 7 illustrates the hourly condensation rate in the EAHE in different months. The condensation rate increases to reach a peak value of about 14.00 before it falls sharply. The condensation rate is strongly affected by the solar radiation profile shown in Figure 8. When the solar radiation increases, the water temperature, and the rate of evaporation also increase, which in turn increases the condensation rate. It is noted that the condensation rate in September is higher than that of March despite the soil temperature in March is the lowest, and the solar radiation is much closed to each other. This is due to the impact of ambient temperature where the maximum values are 28 °C and 46 °C in March and September, respectively.

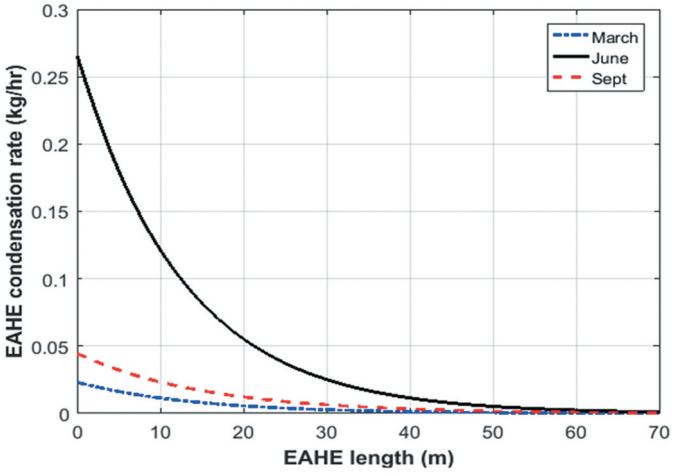

Figure 6. Condensation rate for different months along the earth-air heat exchanger.

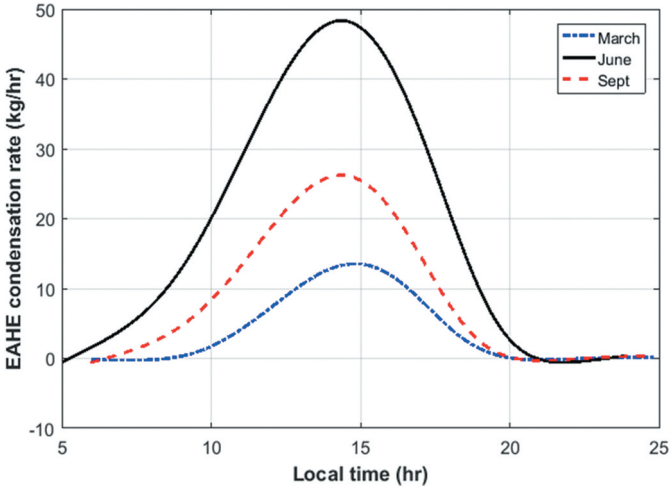

Figure 7. Hourly condensation rate for different months.

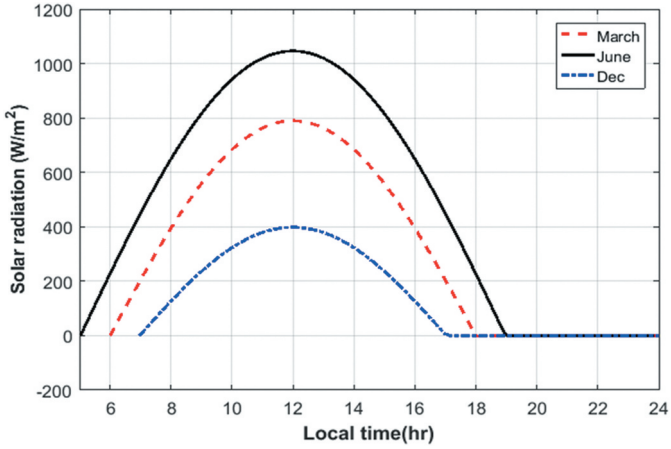

Figure 8. Solar radiation incident on the distiller and the solar chimney for different months.

3.4 Accumulative productivity of freshwater

The daily accumulative condensate along with the length of the solar still and EAHE during March are shown in Figure 9. The solar still has a maximum value of productivity (157 kg) due to the lower ambient and glass temperatures in addition to somewhat high solar intensity (about 800 W/m^2). The accumulative condensate in the EAHE is 76 kg since a part of vapour in the humid air is pre-condensed on the solar still cover before entering the EAHE pipes. In June, the condensation rate in the solar still is approximately zero as it appears in Figure 10; this is due to the high glass temperature, which exceeds the dew point of the humid air. On the other hand, EAHE productivity is higher in comparison with that in March due to the higher evaporation rate and low soil temperature (26 ° C) as well as to the higher moisture content entering the buried pipes, which has not been condensed in the solar still. Figure 11 explains a summary of accumulated productivity throughout the year for both the solar still and the EAHE. In general, the productivity of the EAHE is higher during the summer months due to the high solar intensity, which means a higher evaporation rate, and lower soil temperature, which is lower than the dew point of the humidified air.

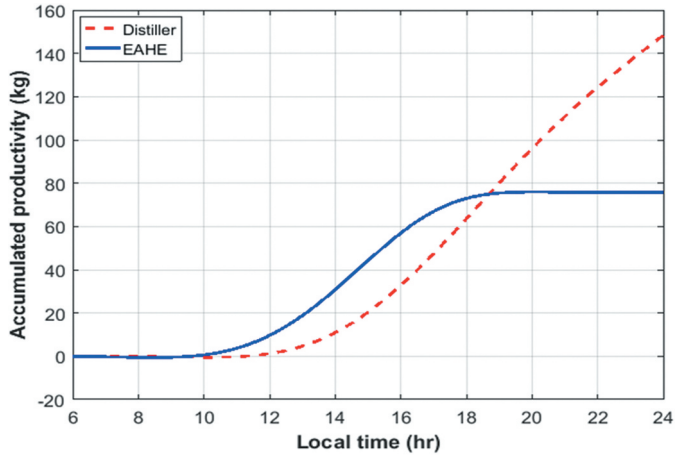

Figure 9. Accumulated productivity of the solar still (distiller) and EAHE with time in March.

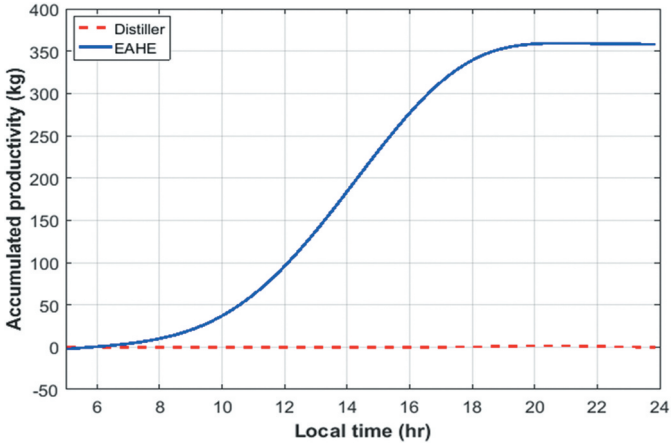

Figure 10. Accumulated productivity of the solar still (distiller) and EAHE with time in June.

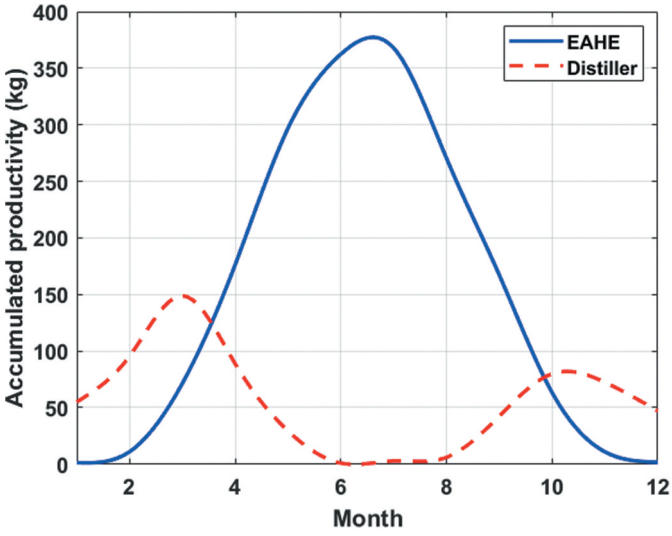

Figure 11. Variation of accumulated productivity of the solar still (distiller) and earth-air heat exchanger around year.

Furthermore, it is noted that the productivity of the solar still is higher in the cold and moderate weather due to the lower glass temperature in comparison with the dew point of the humid air, which enhances the condensation potential. The effect of the soil depth on the monthly accumulative productivity is shown in Figure 12. After a certain depth, it looks no significant impact on productivity. The increase of the depth from 3 m to 5 m increases the average annual productivity by only 2.58%.

3.5 Soil temperature

Figure 13 shows the soil temperature as a function of time and depth (see equation 41). The fluctuation of the soil temperature decreases and the profile tend to be more uniform as the soil depth increases furthermore, the maximum and minimum temperatures are shifted towards the right of the warmest and coldest months (July and January) due to the effect of the heat capacity of the soil.

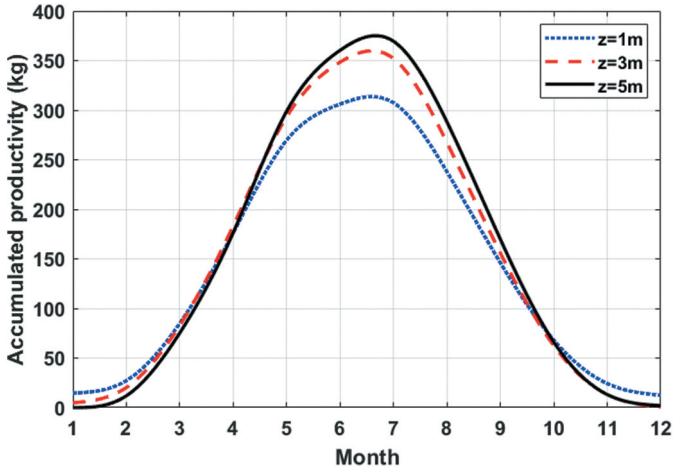

Figure 12. Effect of soil depth on the accumulated productivity throughout the year.

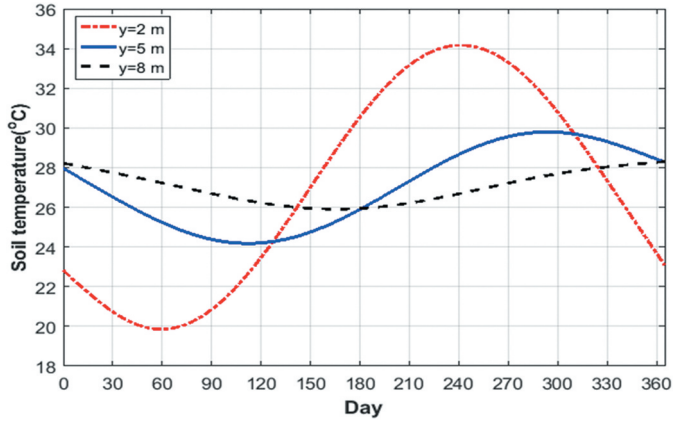

Figure 13. Soil temperature variation for different depths along the year.

3.6 Solar chimney

The updraught air velocity in the solar chimney for different values of the chimney height is explained in Figure 14. The velocity trend is similar to that of the solar radiation incident on the collector also it's seen an increase in the velocity with chimney height due to the rise in the updraught pressure with increasing the chimney height.

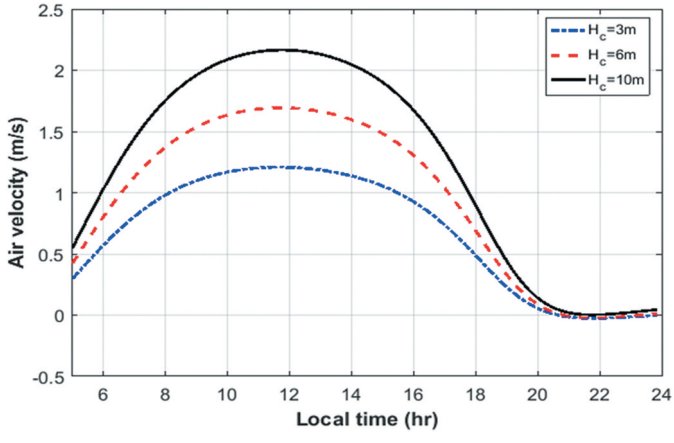

Figure 14. Hourly air velocity profile for different chimney heights.

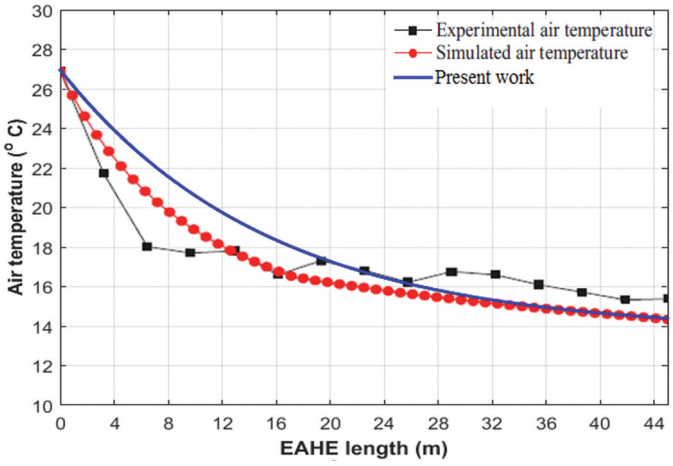

Figure 15. Comparison of the present work and that of Fuxin et al. (2015), (RH_{inlet} = 60%).

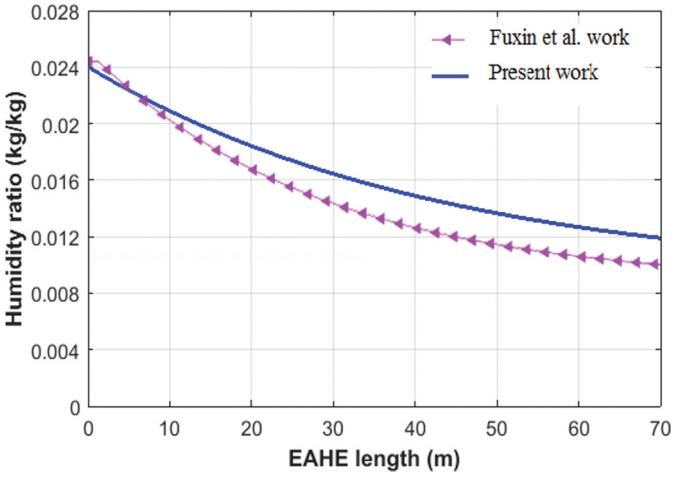

Figure 16. Comparison of the present work and that of Fuxin et al. (2015), (RH_{inlet} = 90%).

3.7 Comparison with the other work

Figures 15 and Figure 16 indicate a comparison of air temperature and humidity ratio in the EAHE between the present work and the work by Fuxin et al. (2015). The inlet parameters (air velocity, soil temperature, and pipe diameter are 1.5 m/s, 12 °C, and 0.5 m, respectively,). The

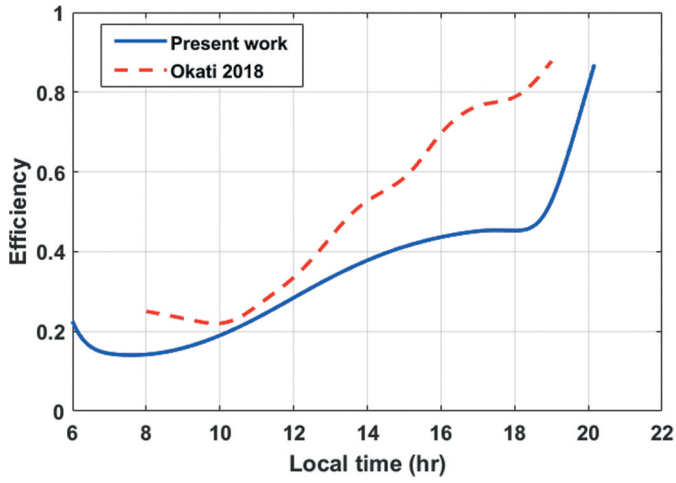

Figure17. Efficiency of the present work and that of Okati et al. (2018)

average percentage differences for air temperature and humidity ratio between the two works are 3.98%, and 11.0%, respectively.

4. System efficiency and cost estimation

Hourly efficiency of the system is the ratio of latent heat released due to condensation of water vapour from the moist air in the solar still and EAHE to the solar radiation incident on the solar still. Mathematically it's given by (Rabhi et al. 2017):

$$\eta = \frac{Productivity of\,(solar still + EAHE)}{Solar energy incident on the solar still} = \frac{(\dot{m}_{co} + \dot{m}_{cp}) \times h_{fg}}{3600 \times I}$$

The hourly efficiency of the system shown in Fig.17 was carried out for July and compared with the work by Okati, Farsad, and Behzadmehr (2018). The efficiency increasing from 0.226 at 6:00 to reach 0.46 at 18:26 before sharp increases to 0.87 just after 20:00. The sharp increase of efficiency is due to the fast-falling of the solar radiation while evaporation and condensation continue due to the thermal inertia of the water in the solar still basin. The difference between the two works is due to the different weather conditions and the soil temperatures. In the present work, the soil temperature is 27.32 °C while it was 17 °C for Okati work.

An economic evaluation was done by using Kabeel, Omara, and Essa (2014) method. The costs of the items used in the system are listed in Table 3. The total fixed cost of the system is

Table 3. Estimation of the system cost.

Item	material	Quantity	Cost per unit/USD	Overall cost /USD
Solar still	Galvanised Iron 2 mm	100 m^2	10	1000
	Glass cover	70,100 m^2	7	700,500,300
	Black paint and material glue	100 m^2	5	
	Insulation		3	
Earth -air heat exchanger	Four galvanised pipes	220 m^2	5	1100
Small Water pump			20	20
Solar chimney	Sand for solar collector base	5 m^3	3	15
	Glass cover	60 m^2	7	420
	PVC pipe (0.25 m diameter)	7	5	35
Installation cost				750
Total fixed cost				4840

estimated to be F = 4840 USD. Assuming that V = 0.3 × F represents variable annual costs and C the total variable and constant costs i.e. C = F + V, if the average life of the equipment used is taken as 10 years, then the total cost is C = 4840 + 0.3 × 10 × 4840 = 19,360 USD. The total daily freshwater yield for the solar still and the EAHE is 207.44 kg. The annual average percentage of sunny days in Basra city through four years 2016–2019 is 90.8%, and therefore the total amount of freshwater produced in the 10 years is:

Amount of fresh water production = 207.44 × 10 × 365 × 0.908 = 687,497.65 kg

Cost of fresh water production (kg) = 19,360/687,497.65 = 0.0282 $

5. Conclusions

A theoretical model of humidification-dehumidification processes in a combination of a solar still and an earth-air heat exchanger with natural air circulation by using a solar chimney is presented. Humidification-dehumidification processes in a transient mode in the whole system are formulated and numerically simulated. It was found that the use of an earth-air heat exchanger is notable for freshwater production from a humidified air and the coupling of a solar still with an earth-air heat exchanger is reliable for continuous freshwater production throughout the year. The maximum productivity of the EAHE occurred within the warm weather, while the solar still has maximum productivity in the cold weather.

The average daily freshwater produced by the entire system throughout the year was 207.44 kg (151.64 kg for the earth-air heat exchanger and 55.8 kg for the solar still). The largest amount of fresh water produced by the entire system (EAHE and solar still) was obtained during the hottest months (June and July) while the minimum productivity was obtained within the coldest months (December and January). The annual productivity of the EAHE was found to be about three times that of the solar still and the condensation rate is greatly dependent on the solar radiation intensity. The humidification and dehumidification processes in the system strongly depend on the solar radiation intensity also the natural air circulation in the system is significantly affected by the solar irradiance as well as the chimney height. No significant effect was found for the soil depth on EAHE productivity after 5 m depth where the soil temperature is reached a uniform value of 27 °C. The average thermal efficiency of the system for the daytime (6:00 to 19:00) was 33.07%.

Nomenclature

A area (m^2)
A_{co} collector area (m^2)
A_p surface area of pipe (m^2)
A_s annual surface temperature amplitude (°C)
A_{ch} chimney cross-section area (m^2)
C_d discharge coefficient (-)
C_{pf} specific heat of air (J/kg°C)
C_w specific heat of water (J/kg°C)
D_{ab} Binary diffusion coefficient (m^2 /s)
D_p EAHE pipes diameter (m)
g gravity acceleration ($m/s^{2)}$
H_{ch} chimney height (m)
h_a heat transfer coefficient between glass and surrounding (W/m^2 °C)
h_w heat transfer coefficient between water and air (W/m^2 °C)
h_f heat transfer coefficient between air and glass (W/m^2 °C)
h_m convective mass transfer coefficient (m/s)
h_{fg} latent heat of evaporation (J/kg)
h_g enthalpy of saturated vapour (J/kg)
h_v enthalpy of vapour (J/kg)
I total solar radiation (W/m^2)
j day of year counted from January 1st
L latitude angle (degree)
$\dot{m}_f$ air mass flow rate (kg/s)
$\dot{m}_{co}$ solar still condensation rate (kg/s)
$\dot{m}_{ev}$ evaporation rate (kg/s)
$\dot{m}_{cp}$ EAHE condensation rate (kg/s)
P atmospheric pressure (N/m^2)
P_g saturated pressure at the glass temperature (N/m^2)
P_f saturated pressure at the air temperature (N/m^2)
P_{ws} saturated pressure at the water temperature (N/m^2)
q_{cg} convection heat transfer between air and glass (W)
q_{cw} convection heat transfer between water and air (W)
q_{ew} evaporative heat transfer between water and air (W)
q_{eg} condensation heat transfer between air and glass (W)
q_{cp} convection heat transfer between air and glass (W)
air and EAHE pipe wall (W)
q_{ep} condensation heat transfer between air and EAHE pipe wall (W)
S day length (m)
Sc Schmidt number
Sh Sherwood number
$T_{a,max}$ monthly maximum ambient temperature (°C)
$T_{a,min}$ monthly minimum ambient temperature (°C)
T_a ambient temperature (°C)
T_{dp} dew point temperature (°C)
T_f airstream temperature (°C)
$\bar{T}_f$ average air temperature (°C)
T_g glass temperature (°C)
T_m average annual soil temperature (°C)
T_w water temperature (°C)
t time (s)
T_p EAHE pipe wall temperature (°C)
T_{co} air temperature in the collector
T_s soil temperature (°C)
t_o time of minimum surface temperature from the start of the year, (hr)
U_a wind velocity (m/s)
U_f airstream velocity (m/s)
w humidity ratio (kg of vapour/kg of dry air)
$\bar{w}_f$ average humidity ratio of air (kg of vapour/kg of dry air)
w_p humidity ratio in EAHE (kg of vapour/kg of dry air)
x solar still horizontal coordinate (m)

y soil depth (m)
z EAHE horizontal coordinate (m)

Greek letters

α_g glass absorptivity (-)
α_w water absorptivity (-)
α_s soil diffusivity (m^2 /s)
β altitude angle (degree)
$\emptyset$ relative humidity (-)
δ declination angle (degree)
ℓ latitude angle (degree)
λ hour angle (degree)
τ_g glass transmissivity (-)

Subscript

f air inside the solar still
g glass
i inlet
o outlet
s saturation
w water

Disclosure Statement

No conflict of interest was reported by the author(s).

Notes on contributor

Dr. ***Salman H. Hammadi***, Professor in mechanical engineering, Basrah University, college of mechanical engineering, Basra, Iraq. Interested field: Renewable energy, Solar desalination, and air conditioning.

References

Abdullah, A. S., M. M. Younes, Z. M. Omara, and F. A. Essa. 2020. "New Design of Trays Solar Still with Enhanced Evaporation Methods – comprehensive Study." *Solar Energy* 203: 164–174. doi:10.1016/j.solener.2020.04.039.

Al-Ajmi, F., D. L. Loveday, and V. I. Hanby. 2006. "The Cooling Potential of Earth–air Heat Exchangers for Domestic Buildings in a Desert Climate." *Building and Environment* 41 (3): 235–244. doi:10.1016/j.buildenv.2005.01.027.

Al-Enezi, F. Q., J. K. Sykulski, and A. A. Nabil. 2011. "Visibility and Potential of Solar Energy on Horizontal Surface at Kuwait Area." *Energy Procedia* 12: 862–872. doi:10.1016/j.egypro.2011.10.114.

Ali, H. M. 1991. "Experimental Study on the Air Motion Effect inside the Solar Still on Still Performance." *Energy Convers Mgmt* 32 (1): 67–70. doi:10.1016/0196-8904(91)90144-8.

Ali, H. M. 1993. "Effect of Forced Convection inside the Solar Still on Heat and Mass Transfer Coefficients." *Energy Convers. Mgmt* 34 (1): 73–79. doi:10.1016/0196-8904(93)90009-Y.

Ali, I. S., A. E. Kabeel, M. M. K. Dawood, A. M. Elharidi, A. B. Elsalam, K. Ramzy, and A. Mehanna. 2020. "Enhancement of the Productivity for Single Solar Still with Ultrasonic Humidifier Combined with Evacuated Solar Collector: An Experimental Study." *Energy Conversion and Management* 208: 112592. doi:10.1016/j.enconman.2020.112592.

Amer, E. H., H. Kotb, G. H. Mostafa, and A. R. El-Ghalban. 2009. "Theoretical and Experimental Investigation of Humidification–dehumidification Desalination Unit." *Desalination* 249 (3): 949–959. doi:10.1016/j.desal.2009.06.063.

Ayman, R. A., and H. Hassan. 2020. "Enhancement of Hybrid Solar Desalination System Composed of Solar Panel and Solar Still by Using Porous Material and Saline Water Preheating." *Solar Energy* 204: 382–394. doi:10.1016/j.solener.2020.04.058.

Bassiouny, R., and N. S. A. Koura. 2008. "An Analytical and Numerical Study of Solar Chimney Use for Room Natural Ventilation." *Energy and Buildings* 40 (5): 865–873. doi:10.1016/j.enbuild.2007.06.005.

Besharat, F., A. A. Dehghan, and A. R. Faghih. 2013. "Empirical Models for Estimating Global Solar Radiation: A Review and Case Study." *Renew. Sustain. Energy Rev* 21: 798–821. doi:10.1016/j.rser.2012.12.043.

Bhargva, M., and A. Yadav. 2020. "Experimental Comparative Study on a Solar Still Combined with Evacuated Tubes and a Heat Exchanger at Different Water Depths." *International Journal of Sustainable Engineering* 13 (3): 218–229. doi:10.1080/19397038.2019.1653396.

Cengel, Y. A., and M. A. Boles. 2001. *Thermodynamics: An Engineering Approach*. 3rd Edition Mcgraw-Hill.

Çengel, Y. A., and A. J. Ghajar. 2015. *Heat and Mass Transfer Fundamentals and Applications*. fifth edition ed. 2 Penn Plaza, New York, NY 10121: McGraw-Hill Education.

Chaabene, M., and M. Annabi. 1997. "A Dynamic Model for Predicting Solar Plant Performance and Optimum Control." *Energy* 22 (6): 567–578. doi:10.1016/S0360-5442(96)00141-7.

De Paepe, M., and A. Janssens. 2003. "Thermo-hydraulic Design of Earth-air Heat Exchanger." *Energy and Building* 35 (4): 389–397. doi:10.1016/S0378-7788(02)00113-5.

El Mghouchi, Y., A. El Bouardi, Z. Choulli, and T. Ajzoul. 2016. "Models for Obtaining the Daily Direct, Diffuse and Global Solar Radiations." *Renew. Sustain. Energy Rev* 56: 87–99. doi:10.1016/j.rser.2015.11.044.

Elango, C., N. Gunasekaran, and K. Sampathkumar. 2015. "Thermal Models of Solar still—A Comprehensive Review." *Renewable and Sustainable Energy Reviews* 47: 856–911. doi:10.1016/j.rser.2015.03.054.

Estrada, E., M. Labat, S. Lorente, and L. A. O. Rocha. 2018. "The Impact of Latent Heat Exchanges on the Design of Earth-Air Heat Exchangers." *Applied Thermal Engineering* 129 (25): 306–317. doi:10.1016/j.applthermaleng.2017.10.007.

Fuxin, N., Y. Yu, D. Yu, and H. Li. 2015. "Heat and Mass Transfer Performance Analysis and Cooling Capacity Prediction of Earth to Air Heat Exchanger." *Applied Energy* 137: 211–221. doi:10.1016/j.apenergy.2014.10.008.

Ghazy, A., and H. E. S. Fath. 2016. "Solar Desalination System of Combined Solar Still and Humidification–dehumidification Unit." *Heat Mass Transfer* 52 (11): 2497–2506. doi:10.1007/s00231-016-1761-1.

Hamed, M. H., A. E. Kabeel, Z. M. Omara, and S. W. Sharshir. 2015. "Mathematical and Experimental Investigation of a Solar Humidification–dehumidification Desalination Unit." *Desalination* 358: 9–17. doi:10.1016/j.desal.2014.12.005.

Hammadi, S. H. 2018. "Tempering of Water Storage Tank Temperature in Hot Climates Regions Using Earth Water Heat Exchanger." *Thermal Science and Engineering Progress* 6: 157–163. doi:10.1016/j.tsep.2018.03.009.

Hassan, E. S. F., S. Elsherbiny, and A. Ghazy. 2004. "A Naturally Circulated Humidifying/dehumidifying Solar Still with A Built-in Passive Condenser." *Desalination* 169 (2): 129–149. doi:10.1016/S0011-9164(04)00521-1.

Incropera, F. P. 2006. *Fundamentals of Heat and Mass Transfer*. 6th edition. Wiley, New York.

Jianliu, X., and L. Weihua. 2013. "Study on Solar Chimney Used for Room Natural Ventilation in Nanjing." *Energy and Buildings* 66: 467–469. doi:10.1016/j.enbuild.2013.07.036.

Kabeel, A. E., Z. M. Omara, and F. A. Essa. 2014. "Improving the Performance of Solar Still by Using Nanofluids and Providing Vacuum." *Energy Conversion and Management* 86: 268–274. doi:10.1016/j.enconman.2014.05.050.

Keshtkar, M., M. Eslami, and K. Jafarpur. 1993. "Effect of Design Parameters on Performance of Passive Basin Solar Stills considering Instantaneous Ambient Conditions: A Transient CFD Modeling." *Solar Energy* 201: 884–907. doi:10.1016/j.solener.2020.03.068.

Lawrence, M. G. 2005. "The Relationship between Relative Humidity and the Dew Point Temperature in Moist Air: A Simple Conversion and Applications." *Bulletin of the American Meteorological Society* 86 (2): 225–233. doi:10.1175/BAMS-86-2-225.

Lindblom, J., and B. Nordell. 2006. "Water Production by Underground Condensation of Humid Air." *Desalination* 189 (1–3): 248–260. doi:10.1016/j.desal.2005.08.002.

Lindblom, J., and B. Nordell. 2007. "Underground Condensation of Humid Air for Drinking Water Production and Subsurface Irrigation." *Desalination* 203 (1–3): 417–434. doi:10.1016/j.desal.2006.02.025.

Mawire, A., and M. McPherson. 2008. "Experimental Characterization of a Thermal Energy Storage System Using Temperature and Power Controlled Charging." *Renewable Energy* 33 (4): 682–693. doi:10.1016/j.renene.2007.04.021.

Mohamed, A. S. A., A. G. Shahdy, and M. S. Ahmed. 2021. "Investigation on Solar Humidification Dehumidification Water Desalination System Using a Closed-air Cycle." *Applied Thermal Engineering* 188: 116621. doi:10.1016/j.applthermaleng.2021.116621.

Molineaux, B., B. Lachal, and O. Guisan. 1994. "Thermal Analysis of Five Outdoor Pools Heated by Unglazed Solar Collectors." *Solar Energy* 53 (1): 21–26. doi:10.1016/S0038-092X(94)90599-1.

Okati, V., A. Behzadmehr, and S. Farsad. 2016. "Analysis of a Solar Desalinator (Humidification–dehumidification Cycle) Including a Compound System Consisting of a Solar Humidifier and Subsurface Condenser Using DoE." *Desalination* 397: 9–21. doi:10.1016/j.desal.2016.06.010.

Okati, V., S. Farsad, and A. Behzadmehr. 2018. "Numerical Analysis of an Integrated Desalination Unit Using Humidification-dehumidification and Subsurface Condensation Processes." *Desalination* 433: 172–185. doi:10.1016/j.desal.2017.12.029.

Ozgener, O., L. Ozgener, and J. W. Tester. 2013. "A Practical Approach to Predict Soil Temperature Variations for Geothermal (Ground) Heat Exchangers Applications." *International Journal of Heat and Mass Transfer* 62: 473–480. doi:10.1016/j.ijheatmasstransfer.2013.03.031.

Rabhi, K., R. Nciri, F. Nasri, C. Ali, and H. B. Bacha. 2017. "Experimental Performance Analysis of a Modified Single-basin Single-slope Solar Still with Pin Fins Absorber and Condenser." *Desalination* 416: 86–93. doi:10.1016/j.desal.2017.04.023.

Reicosky, D. C., L. J. Winkelman, J. M. Baker, and D. G. Baker. 1989. "Accuracy of Hourly Air Temperatures Calculated from Daily Minima and Maxima." *Agricultural and Forest Meteorology* 46 (3): 193–209. doi:10.1016/0168-1923(89)90064-6.

Rogers, R. R., and M. K. Yau. 1989. *A Short Course in Cloud Physics*. Pergamon Press.

Sartori, E. 1996. "Solar Still versus Solar Evaporator: A Comparative Study between Their Thermal Behaviors." *Solar Energy* 56 (2): 199–206. doi:10.1016/0038-092X(95)00094-8.

Sartori, E. 2006. "Convection Coefficient Equations for Forced Airflow over Flat Surfaces." *Solar Energy* 80 (9): 1063–1071. doi:10.1016/j.solener.2005.11.001.

Sharshir, S. W., G. Peng, N. Yang, M. A. Eltawil, M. K. Ahmed Ali, and A. E. Kabeel. 2016. "A Hybrid Desalination System Using Humidification-dehumidification and Solar Stills Integrated with Evacuated Solar Water Heater." *Energy Conversion and Management* 124: 287–296. doi:10.1016/j.enconman.2016.07.028.

Sivaram, P. M., S. Dinesh Kumar, M. Premalatha, T. Sivasankar, and A. Arunagiri. 2021. "Experimental and Numerical Study of Stepped Solar Still Integrated with a Passive External Condenser and Its Application." *Environment, Development and Sustainability* 23 (2): 2143–2171. doi:10.1007/s10668-020-00667-4.

Zanganeh, P., A. S. Goharrizi, S. Ayatollahi, M. Feilizadeh, and H. Dashti. 2020. "Efficiency Improvement of Solar Stills through Wettability Alteration of the Condensation Surface: An Experimental Study." *Applied Energy* 268: 114923. doi:10.1016/j.apenergy.2020.114923.